Optimized Yield Curve Determination Using Bulge Test Combined with Optical Measurement and Material Thickness Compensation

Harald Friebe[1,a], Markus Klein[1,b], Ingo Heinle[2,a], Arnulf Lipp[2b]

[1]GOM mbH Mittelweg 7-8, 38106 Braunschweig, Germany

[2]BMW Group, München, Germany

[a]h.friebe@gom.com, [b]m.klein@gom.com,

[c]ingo.heinle@bmw.de [d]arnulf.la.lipp@bmw.de

Keywords: Flow curve; material modeling; bulge test; forming simulation; optical strain measurement

Modeling the behavior of plastic hardening requires an accurate yield curve, which is typically determined by performing a tensile test. As long as the specimen is uniformly elongated one can assume that a uniaxial stress state is induced. Due to this limitation the maximum accumulated plastic strain evaluated from standard tensile tests is lower than that for deep drawing processes for industrial sheet metal components. The bulge test offers experimental data for modeling the plastic hardening behavior at more elevated strain levels. The yield curve evaluated from bulge tests is usually derived by utilizing the membrane theory. The evaluation of the strain state, which is needed for the computation of the material thickness, and the knowledge about the curvature at the top of the dome is necessary for the determination of the flow curve. Nowadays [1], optical measuring systems like ARAMIS are utilized for measurements of the time dependent deformation field. The exploitation of the measured data enables the computation of the associated thickness and the curvature at the top of the dome with respect to the measured surface. For the values of the curvature and the pressure the membrane theory refers to the mid-surface of the material. The thickness must be small relative to the radius of curvature. For materials where the thickness might be several millimeters this assumption could lead to a deviation between theoretical results and real material response. The pressure acts at the inner surface but the strain state and the curvature are typically derived from the visible outer surface of the test specimen. Consequently, the curvature and the pressure do not refer to the mid-surface, as needed for the application of the membrane theory,. In this paper different methods for compensating the aforementioned issues will be discussed. As opposed to the first experimental comparison in [2] the validation of the different approaches is carried out by an extensive forming simulation of the bulge test. A predefined yield curve is used in the applied material model. The computed deformation field of the simulation is processed in the same way as the experimental data of the bulge test. Finally, the comparison of the recalculated yield curve with the predefined one allows a benchmark of different aspects of the mentioned compensation strategies.

Introduction

Axisymmetric die and binder are typically used in the bulge test, where the test specimen is formed by increasing the level of oil pressure (Fig. 1). With this experimental setup a biaxial stress state is induced at the specimen dome, assuming that it is not influenced by friction. The increasing oil pressure in the region of the top of the dome is recorded and the deformation field measured during the forming process. The optical measurement system determines the coordinates, the deformations and the curvature on the outer surface. Based on the forthcoming ISO 16808 these results are directly used for the calculation of the flow curve. In order to determine the flow curve based on the bulge test, an analytical approach is needed for the computation of the stress state at the top of the dome.

Bending stresses can be neglected [4], if the ratio between the sheet metal thickness and the bulge diameter is small and consequently the requirements for deploying the membrane theory for the determination of the biaxial stress state are fulfilled:

$$\sigma_B = \frac{p\rho}{2t} \tag{1}$$

As shown by expression (1), the biaxial stress state at the top of the dome depends on the materials current thickness t, the oil pressure p and the radius of the dome ρ at the corresponding location. The quantities ρ and p refer to the middle layer. Eq. 1 is derived by assuming that both principal stresses are equal ($\sigma_B=\sigma_1=\sigma_2$) [5]. Additionally, the shape of the dome in the pole zone is assumed to be spherical. By assuming the plastic incompressibility the thickness can be computed based on the measured major and minor strain values (ε_1, ε_2)

$$t = t_0 e^{\varepsilon_3}, \quad \varepsilon_3 = -(\varepsilon_1 + \varepsilon_2). \tag{2}$$

A forming simulation of the bulge test is performed, as described by Volk et al. [4]. They suggested a validation procedure utilizing numerical simulation methods to investigate the usability of the membrane theory for the calculation of the biaxial stress state. The nodal coordinates from different points in time during the forming process, representing the geometry of the test part, are calculated. The time dependent positions of these points describe the deformation of the specimen during the forming operation. Finally, these points resulting from the simulation are treated in the same way as an experimentally determined deformation field (Fig. 1).

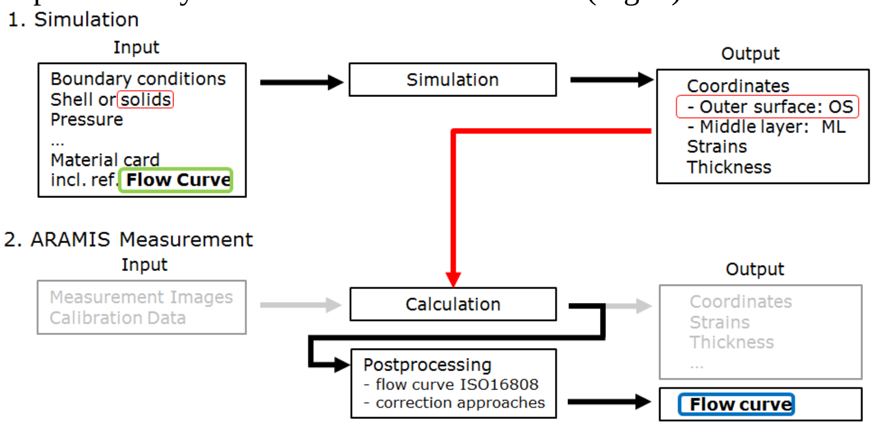

Fig. 1 *– Computation procedure for the validation of a recalculated flow curve based on a forming simulation and the initial “reference” flow curve*

Based on the exported point sets and the pressure progression, the algorithm for the determination of the flow curve should be able to reproduce the flow curve, if an isotropic material model is deployed. The reference surface of the shell elements, as described in [4], are coincident with the middle layer. Consequently, the requirements of Eq. 1 are fulfilled. Volk et al. [4] showed that the membrane theory is applicable for sheet metal thicknesses of 0.5 mm, 1.0 mm and 3.0 mm (for d_{die} = 200 mm).

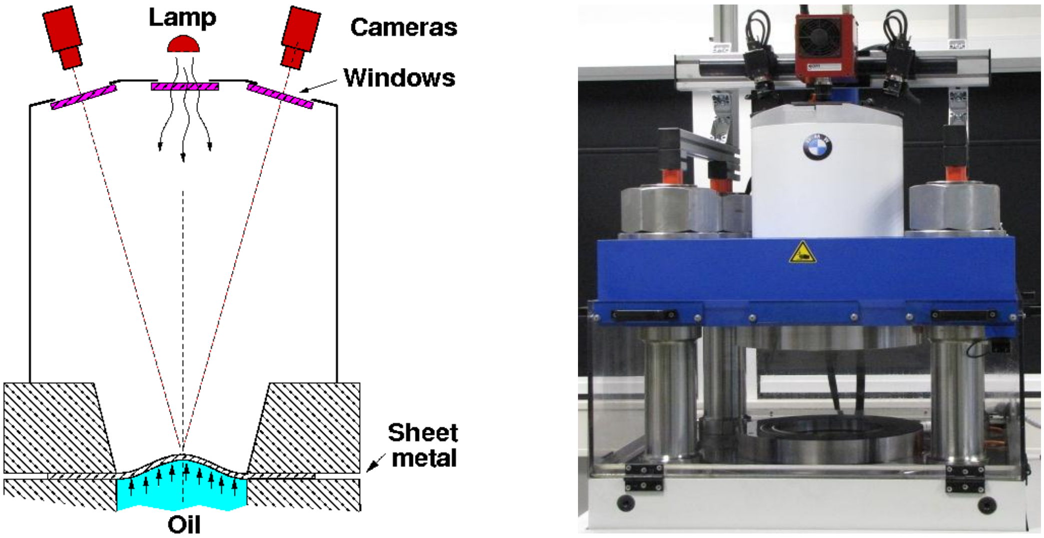

Fig. 2 *– Principle and experimental setup of the laboratory of BMW using the optical measuring system ARAMIS*

Correction proposals for the flow curve calculation

As discussed before, the results of the system for measuring the time dependent deformation field refers to the visible surface (outer surface) and the pressure acts on the opposite side (inner surface). Therefore, the requirements of Eq. 1 are not fulfilled as the measured quantities do not refer to the middle layer. There might be negative side effects if this discrepancy is neglected. However, it might be possible to relate the measured quantities to the middle layer by applying suitable compensation strategies. In [2,7] such strategies are discussed further.

Compensation for bending effects

Approach – S. The ARAMIS system provides a function called “material thickness compensation”, which shifts the measured surface coordinates to values at the middle layer m of the blank. By applying this function the strain field is calculated according the shifted surface coordinates, referring to the middle layer. This procedure eliminates the bending influence in the strain field based on the local curvature. As a result a new strain field (ε_{1m}, ε_{2m}) is obtained, which defines a bending compensated strain field and consequently allows an improved computation of the material thickness according to Eq. 2.

Approach - S*. In [7] a simplified approach for the compensation of the bending effect is shown.

$$t_m = t_0 e^{\varepsilon_{3m}}, \quad \varepsilon_{3m} = \varepsilon_3 - 2\ln\left(1 - \frac{t_0}{2\rho} e^{\varepsilon_3}\right), \quad \varepsilon_3 = -(\varepsilon_1 + \varepsilon_2)\,. \tag{3}$$

Influence of the material thickness on curvature determination.

Approach – R. By using the above mentioned function (material thickness compensation), the curvature can be computed with respect to the middle layer coordinates.

Approach – R*. A simplified method for an improved computation of the curvature is given in [2,7]:

$$\rho_m^* = \rho_s - \frac{t_m}{2}\,. \tag{4}$$

In [2] a significant deviation between these two methods is reported. According to this study, approach R is preferred, as the simple approach does not take the local thinning at the apex of the dome into account. As a consequence, the simple approach does not give reasonable results for the real radius of the middle layer ρ_m for higher strain values. Fig. 3 shows the fundamental difference between the real ρ_m under consideration of localized thinning and ρ_m^* calculated without taking localized thinning into account.
The radius ρs of the outer layer is depicted by using a constant value. Considering that a homogeneous thinning of the material occurs this simple approach can be applied (left hand side). The effect of considering localized thinning is shown on the right hand side. One can observe that ρm is much smaller than ρm* from the left hand side. Thus the simplified approach cannot be applied in the case of localized thinning.

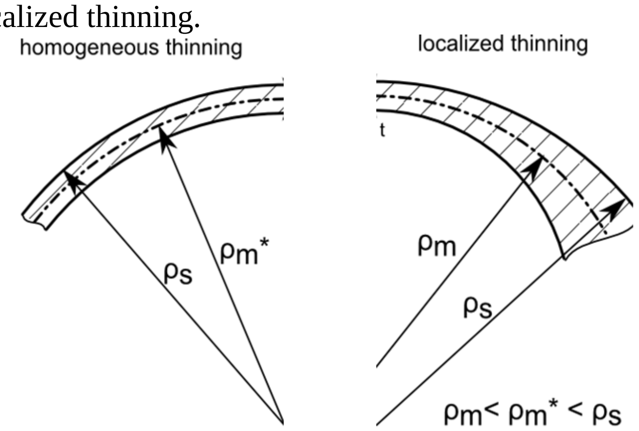

Fig. 3: *Real ρ_m for the case of localized thinning defined by middle layer coordinates (right side) in comparison to simple approach by (Eq. 4), which is only valid for homogenous thinning (left side) [2]*

Compensation of the pressure. *Approach – P.*
As the pressure acts on the inner layer of the material, in [2,7] a simple compensation approach is proposed in order to consider the discrepancy between the assumption of Eq.1 and the experimental setup. The compensation strategy is derived from the general balance of forces for thin shells (see Eq. 1). Eq. 5 is formulated for application in combination with the correction methods R and S. If other compensation strategies should be applied, the pressure compensation must be suitably adapted

$$\sigma = \frac{p \cdot \rho_m}{2t_m} \cdot \left(1 - \frac{t_m}{2\rho_m}\right)^2 . \tag{5}$$

Elastic strain compensation. *Approach – E.*
Usually only the plastic part of the strain state is needed for modeling the hardening effect. For determining the plastic part of the strain state a compensation of the elastic strain state is proposed in [7] by using the Hooke's law comprising the model parameters Young's modulus and Poisson's ratio.

Procedure for investigating compensation strategies

For an assessment of the different compensation strategies the real flow curve should be known. Unfortunately the real flow curve is unknown. As shown above [4], it is possible to investigate the mentioned correction methods based on simulation studies. To enable the extraction of the corresponding nodal displacements on the outer surface of the specimen and allow the definition of a pressure boundary condition acting on the inner surface, volume elements (solids) are used (Fig. 4). By applying this type of element, it is possible to reflect the mentioned conditions of the real experiments. To avoid a reduction in accuracy of the numerical integration [6], the initial blank comprises cubic shaped volume elements. The forming simulations are performed by using a hypo elasto-plastic material model. The hardening is assumed to be isotropic and a von Mises yield locus is selected. For an increasing material thickness the significance of the mentioned discrepancy regarding the application of Eq. 1 is expected to rise. The investigations of this study are performed on the basis of the upper limit of the material thickness according to the forthcoming ISO 16808, which is given by $t_0 \leq d_{die}/33$. The investigations are aligned to the experimental setup of the laboratory of BMW (Fig. 2) comprising a die diameter of $d_{die} = 200mm$. By applying $t_{\max} = d_{die}/33$ a maximum sheet thickness of $t_{\max} = 6mm$ is permissible.

The investigations, which are shown below, are based on this maximum sheet thickness in combination with a flow curve derived from the interstitial free mild steel DX54.
For the validation of the different approaches the results of the simulation (time dependent nodal coordinates and the pressure progression) are used to calculate a new flow curve. The recalculated curve can be compared with the curve of the material card as shown in Fig. 1.

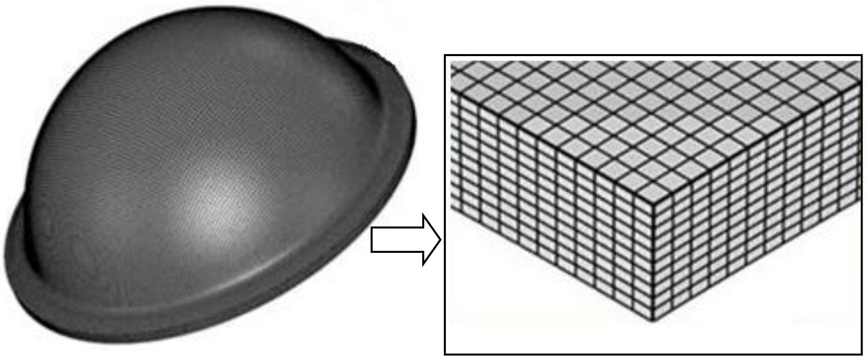

Fig. 4 *– Forming simulation of bulge test using volume elements*

Validation of the applicability of the membrane theory

The investigations of Volk et al. [4] are limited to a maximum sheet thickness of 3mm. As a consequence, the applicability of the membrane theory is studied again on the basis of a sheet thickness of 6mm. The volume elements, applied in this study, also enable the exporting of the deformation field on the middle layer. The definition of the pressure boundary condition is not limited to the inner surface. Thus the pressure boundary condition is defined according to the membrane theory. Therefore, the simulation model complies with all the requirements for applying the membrane theory.
A comparison between the flow curve of the material card “Ref” (reference curve) and the recalculated flow curve “ML” (ML: middle layer) is shown in Fig. 5. The flow curve “ML-E” is calculated by adding the compensation of the elastic strains based on approach E.

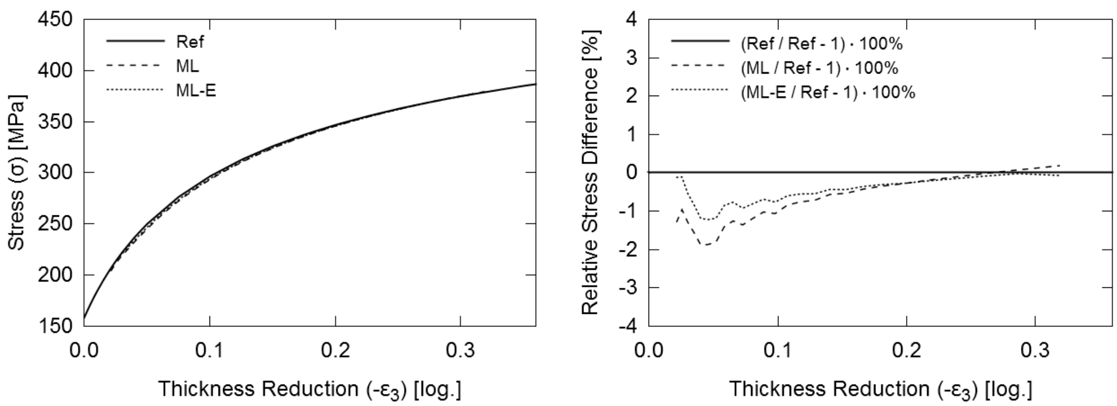

__Fig. 5:__ Comparison of Ref (flow curve from the material card), ML (recalculated flow curve based on Eq. 1 with respect to the middle layer) and ML-E (recalculated flow curve without the elastic strains). (a): original stress values, (b): relative stress deviation to Ref

The left graph of Fig. 5 does not show any significant deviation between the different flow curves. The relative deviations between the recalculated curves and the reference curve are given by the right graph of Fig. 5. The validity of the membrane theory for the determination of the biaxial stress state at the top of the dome is confirmed by the recalculated curve (maximum deviation: 2%). By additionally eliminating the elastic part of the strain state (curve "ML-E" in Fig. 5), the deviations are reduced regarding the whole curve and the maximum deviation is approximately 1% (in the zone of low strain levels). The compensation of the elastic part should be reasonable as the flow curve of the material card is defined without the elastic part of the strain state. This expectation is confirmed by the curves "Ref" and "ML-E" in Fig. 5.

Validation of the correction approach concerning the pressure. *Approach – P*

Approach P (compensation of pressure acting on the inner surface) should be validated with a second simulation. Based on the same type volume elements the pressure boundary condition is defined in this case so that the pressure acts on the inner surface.

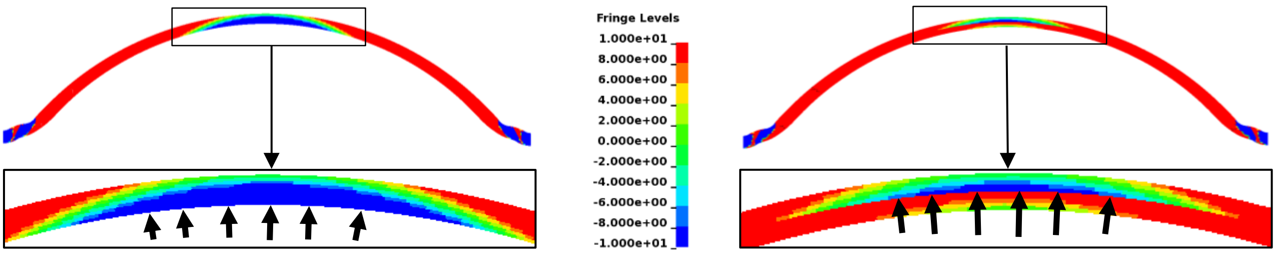

__Fig. 6:__ Calculated stress in z-direction (normal to surface of pole) for pressure acting on the inner surface (left) and acting on the middle layer (right)

For both simulations (pressure on inner surface and on middle layer) the shape of the middle layers surface is compared for similar deformation states. The deviation of the shape (difference in z-direction) is shown in Fig. 7. The maximum deviation is -19*µm* at the edges and -15*µm* in the center. Understanding the -15*µm* of the center as an offset, the curvature of the shape differs less than 4µm for the presented area in a size of approx.60x60mm.

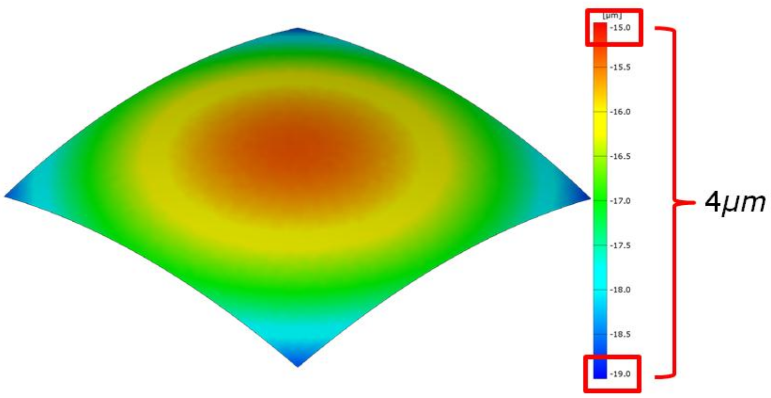

__Fig. 7:__ Surface deviation in z-direction (normal to surface of pole) for pressure acting on the inner surface and acting on the middle layer

The deformation fields of the corresponding points on the middle layer are used for both simulations to recalculate the flow curve. Additionally for the simulation with pressure on the inner layer a flow curve ML_{Pi}-P is recalculated using approach P**.** The results are shown in Fig. 8.

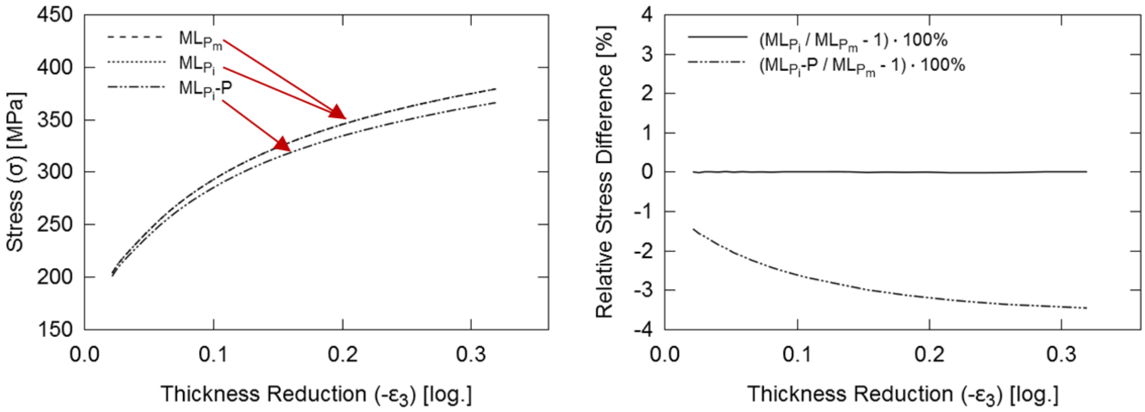

Fig. 8: *Comparison of recalculated flow curves for pressure acting on the inner surface ML_{Pi}, for pressure acting on the middle layer ML_{Pm} and for the inner layer using approach P (ML_{Pi}-P); (a): original stress values, (b): relative stress deviation to ML_{Pm}*

A difference between ML_{Pi} (acting on the inner surface) and ML_{Pm} (acting on middle layer) is not recognizable (see Fig. 8). The relative stress difference is negligible. However, if approach P is used, a large relative difference occurs (>1,5…3%). Contrary to the suggestion in [2,7] this result indicates that it is not useful to compensate the pressure acting on the inner surface for the case of materials with larger thickness.

Validation of the correction approaches concerning the strain state and the curvature ***Approaches S, S*, R, R****

The same simulation as shown before is used for the validation of the other compensation approaches, too. In order to be comparable to a real measurements, the deformation fields of corresponding points on the outer surface (OS) are used to recalculate the flow curve. The flow curve ML is recalculated on the middle layer coordinates (equal to Fig. 5) and is used as a target for the correction. The different approaches (S, S*, R, R*) are used to compensate the flow curve correction based on OS and the results are shown in Fig. 9.

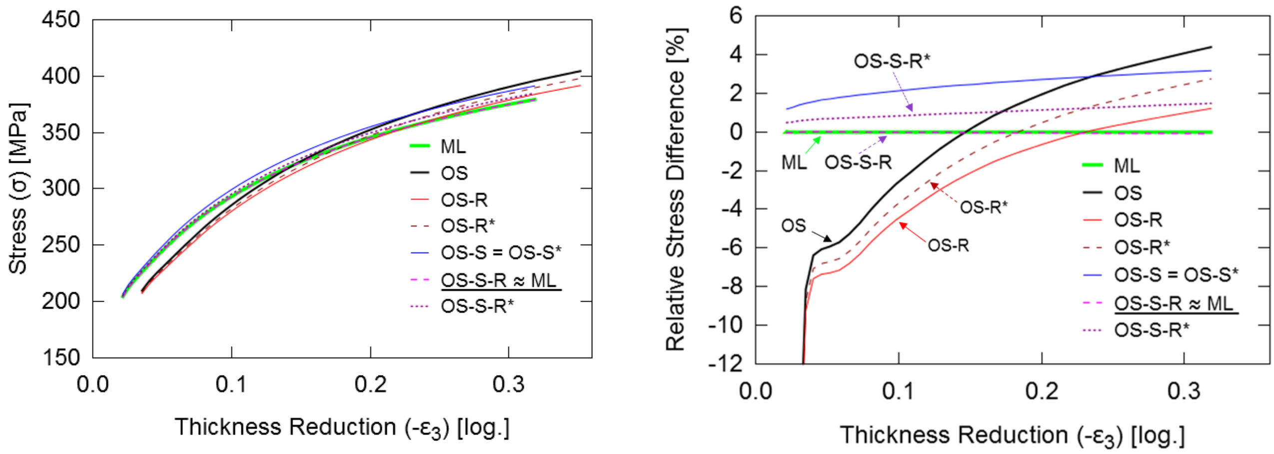

Fig. 9: *Comparison of recalculated flow curves: (a): ML reference curve based on middle layer data, (b): OS outer surface data with different added approaches. OS-S-R overlies ML (material thickness t=6mm, punch d_{die} = 200mm)*

Approach S and S* deliver comparable results (no difference visible in Fig. 9, right graph). The flow curve OS-S-R overlays ML. Thus the combination of S and R (or S* and R) seems to be the optimal correction and an additional correction of the pressure is not required. If the optical measuring system ARAMIS is used the thickness compensation S and R can be performed together. In comparison to correction R, the correction R* underestimates the influence of local thinning for the whole curve.

Typically a flow curve should represent only the plastic part of the strain state. Thus curves in Fig. 9 must be additionally corrected by using approach E. This will modify OS-S-R of Fig. 9 similar to ML in Fig. 5.

Summary

According to the forthcoming ISO 16808 this investigation confirms the applicability of the membrane theory for the maximum permissible sheet thickness regarding a die diameter of $d_{die} = 200mm$.

As shown in this paper, the discrepancies between the experimental setup and the requirements of the membrane theory can affect the quality of experimentally determined flow curves.

The presented simulation and validation results show that the influence on the flow curve based on the material thickness can be eliminated using the above described approaches R and S or S*, even for thick sheet metal blanks.

The evaluations of the numerical forming simulations seems to show that the pressure compensation (approach P) on the acting surface is not useful and should not be considered for the determination of flow curves.

References

[1] S. Keller et al., Experimental Procedure in Yield Curve Determination Using the Bulge Test combined with Optical Measurement, Proceedings of IDDRG 2009 International Conference, Golden, CO, USA, pp. 319-330.

[2] M.Vucetic et al., Numerical Validation of Analytical Biaxial True Stress – True Strain Curves From the Bulge Test, AIP Conf. Proc. 1383, pp. 107-114, The 8th International Conference and Workshop on Numerical Simulation of 3D Sheet Metal Forming Processes (NUMISHEET 2011), 2011, Seoul, Republic of Korea

[3] W. Panknin, Der hydraulische Tiefungsversuch und die Ermittlung von Fließkurven, PhD thesis, Technische Hochschule Stuttgart, 1959.

[4] W. Volk, I. Heinle and H. Grass. Accurate Determination of Plastic Yield Curves and an Approximation Point for the Plastic Yield Locus with the Bulge Test, In Proceedings of the 10th International Conference on Technology of Plasticity, ICTP, 2011 pp. 799-804.

[5] A.D. Santos, P. Teixeira, A. Barata da Rocha and F. Barlat. On the Determination of Flow Stress Using Bulge Test and Mechanical Measurement, In NUMIFORM 2010: Proceedings of the 10th International Conference on Numerical Methods in Industrial Processes, 2010, pp. 845-852.

[6] K.-J. Bathe. Finite-Elemente-Methoden (Aus dem Englischen übersetzt von Peter Zimmermann). Springer Verlag, second edition, 2002.

[7] Leppin et al., Evaluation of the Hydraulic Bulge Test for Improved Material Hardening Modeling, Proceedings of 5th Forming Technology Forum Zurich 2012: Advanced Failure Prediction Methods in Sheet Metal Forming, 2012, Zürich, Switzerland, ISBN 978-3-906031-06-4, pp. 69-74